Targeted Narrowband Intense Pulsed Light on Cutaneous Vasculature

Wesley J. Moy,[1,2] Joshua D. Yakel,[1] O. Cecilia Osorio,[1] Jocelynda Salvador,[1] Carole Hayakawa,[1,3] Kristen M. Kelly,[1,4,5] and Bernard Choi[1,2,5,6]*

[1]*Beckman Laser Institute and Medical Clinic, University of California, Irvine, California*
[2]*Department of Biomedical Engineering, University of California, Irvine, California*
[3]*Department of Chemical Engineering and Materials Science, University of California, Irvine, California*
[4]*Department of Dermatology, University of California, Irvine, California*
[5]*Department of Surgery, University of California, Irvine, California*
[6]*Edwards Lifesciences Center for Advanced Cardiovascular Technology, University of California, Irvine, California*

Background and Objectives: Laser based therapies are the standard treatment protocol for port wine stain in the United States, but complete removal is infrequently achieved. Intense pulsed light (IPL) offers a broadband light spectrum approach as a viable treatment alternative. Previous studies suggest that IPL can be more effective in treatment of port wine stain by utilizing multiple wavelengths to selectively target different peaks in oxy- and deoxy-hemoglobin. Our study objectives were to (i) determine a characteristic radiant exposure able to achieve persistent vascular shutdown with narrowband IPL irradiation, (ii) determine the degree to which narrowband IPL irradiation can achieve persistent vascular shutdown, and (iii) compare the effectiveness of narrowband IPL radiation to single wavelength pulsed dye laser (PDL) irradiation in achieving persistent vascular shutdown.

Study Design/Materials and Methods: We utlized either single pulse or double, stacked pulses in narrowband IPL experiments, with the IPL operating over a 500–600 nm wavelength range on the rodent dorsal window chamber model. We compared the results from our narrowband IPL experiments to acquired PDL data from a previous study and determined that narrowband IPL treatments can also produce persistent vascular shutdown. We ran Monte Carlo simulations to investigate the relationship between absorbed energy, wavelength, and penetration depth.

Results: For single and double pulse narrowband IPL irradiation we observed (i) little to no change in blood flow, resulting in no persistent vascular shutdown, (ii) marked acute disruption in blood flow and vascular structure, followed by partial to full recovery of blood flow, also resulting in no persistent vascular shutdown, and (iii) immediate changes in blood flow and vascular structure, resulting in prolonged and complete vascular shutdown. Monte Carlo modeling resulted in a 53.2% and 69.0% higher absorbed energy distribution in the top half and the total simulated vessel when comparing the composite narrowband IPL to the 595 nm (PDL), respectively.

Conclusions: Our data collectively demonstrate the potential to achieve removal of vascular lesions using a 500–600 nm range. Additionally, the narrowband IPL was tuned to optimize a specific wavelength range that can be used to treat PWS, whereas the PDL can only operate at one discrete wavelength. Lasers Surg. Med. 47:651–657, 2015. © 2015 Wiley Periodicals, Inc.

Key words: Laser speckle imaging; Photothrombosis; Photocoagulation; Selective; photothermolysis

INTRODUCTION

Port Wine Stains (PWS) are vascular malformations of the skin that are birthmarks. PWS are characterized by an increase in vessel diameter (vasodilation) and increase in the number of blood vessels (hypervascularization) [1]. PWS lesions initially present as a reddish pink coloration of the skin and are flat in nature. If left untreated, PWS often develop nodules and tissue hypertrophy [2], and can lead to dental abnormalities and psychosocial problems [3].

The standard treatment in the United States of PWS utilizes high intensity light, typically delivered by a laser, to selectively target abnormal vasculature. Clinicians often use the pulsed dye laser (PDL, $\lambda = 585$–595 nm), in conjunction with epidermal cooling [4], to minimize the amount of surrounding tissue damage caused by the thermal energy of the laser. The PDL is selectively absorbed by oxy- and deoxy-hemoglobin in blood vessels [3,5] and subsequently is converted to heat that ideally

Contract grant sponsor: National Institutes of Health; Contract grant number: R01HD065536; Contract grant sponsor: National Institutes of Health Laser Microbeam; Contract grant number: P41EB015890; Contract grant sponsor: Medical Program; Contract grant number: NIH K25-EB007309.

*Correspondence to: Bernard Choi, Ph.D., University of California, Irvine, Beckman Laser Institute and Medical Clinic, 1002 Health Sciences Road East, Irvine, CA 92612.
E-mail: choib@uci.edu

Accepted 22 June 2015
Published online 31 July 2015 in Wiley Online Library (wileyonlinelibrary.com).
DOI 10.1002/lsm.22393

reaches temperatures that create localized damage. Subsequent thrombosis formation leads to either a severe reduction in or shutdown of blood flow [6]. This entire treatment protocol is known as selective photothermolysis [7].

While PDL therapy of PWS has led to successful lightening of the PWS color, patients may require several laser treatments [8] before seeing sufficient improvement. Consistent PDL treatments can span several years, depending on the severity of the PWS disease, and its resistance to the PDL treatment. Furthermore, PDL therapy is not as effective for PWS patients with darker skin due to the competitive absorption of the laser light by epidermal melanin. As a result, the maximum radiant exposure must be decreased in consideration of tissue damage and safety concerns, which in turn limits the effectiveness of laser treatment.

Here, we investigated the use of targeted narrowband intense pulsed light (IPL) as an alternative light source to the PDL to determine if a range of wavelengths is more effective than the single wavelength from the PDL. A previous study of PDL-resistant PWS [9] suggested that IPL could be used as an alternative to the PDL. In this study, all subjects ($n = 15$), with PWS of various sizes, locations and colors, achieved at least a 50% reduction of their PWS through IPL treatments. Another study conducted in China investigated the treatment of 30 PWS patients with IPL [10], with 3–8 treatment sessions over a duration of 4–5 weeks. They reported that 100% of patients showed more than 25% clearance, while 30% of patients were able to achieve 75% clearance, further showing that IPL, under certain treatment parameters, has the potential to be an effective treatment for PWS clearance both in terms of a reduction in the number of treatments and improved efficiency of the each treatment. A split-face study performed using the PDL and IPL [11] demonstrated that an IPL with a wavelength range of 555–950 nm achieved more effective clearance than the PDL ($\lambda = 585$ nm). Additionally, data from other studies [12,13] suggest that IPL is a viable option for PWS clearance, but acknowledge that, due to the large variance in treatment parameters (pulse duration, radiant exposure, wavelength range), IPL warrants further investigation.

In this study, we used a narrowband IPL that emits broadband light over the wavelength range of 500–600 nm. The wavelength range of this narrowband IPL enables light absorption over the entire absorption spectra of oxy- and deoxy- hemoglobin, including the 577 and 600 nm oxyhemoglobin absorption peaks, which may enhance PWS clearance [14]. The objectives of the current study were to (i) determine a characteristic radiant exposure able to achieve persistent vascular shutdown with narrowband IPL irradiation, (ii) determine the degree to which narrowband IPL irradiation can achieve persistent vascular shutdown, and (iii) compare the effectiveness of narrowband IPL radiation to single wavelength PDL irradiation in achieving persistent vascular shutdown.

MATERIALS AND METHODS

Dorsal Window Chamber Model

Similar to previous work from our group [15,16], we utilized the dorsal window chamber model [17] and performed experiments on adult C3H mice (25–30 g, $n = 41$). All experiments were approved by the Institutional Animal Care and Use Committee at University of California, Irvine.

IPL Irradiation

For narrowband IPL irradiation, we utilized a commercially available IPL (Dye-VL, Alma Lasers US, Buffalo Grove, IL) with a spot size of 10 mm, pulse duration between 3 and 5 ms and radiant exposure between 7 and 15 J/cm^2. A 15 mm diameter, 1–2 mm thickness of ultrasound gel was placed on the epidermal side of the window chamber, prior to contact with IPL device. Figure 1 shows the variable intensity as a function of wavelength, specific to this IPL device.

Experimental Design

We anesthetized and positioned the animal in a custom window chamber holder placed on top of a heating pad. We irradiated the window chamber from the epidermal side with either a single pulse or two stacked pulses of narrowband IPL. For the latter (i.e., double-pulse) narrowband IPL experiments, a one-second delay was used between administration of the first and second pulses. All experiments were randomized to minimize systematic bias.

Laser Speckle Imaging (LSI)

We monitored the photothermal effects of the IPL irradiation by observing blood flow dynamics using LSI. Briefly, a 633 nm Helium-Neon laser was used to a illuminate the dermal side of the window chamber, from which raw speckle image sequences were collected. Using a

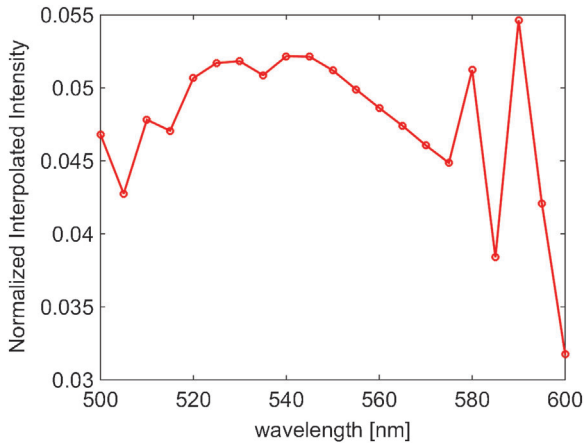

Fig. 1. Interpolated output pectrum of Alma Dye-VL IPL device at the wavelengths used in the Monte Carlo simulations. Note that the line connecting the data points is included as a guide, and does not represent the shape of the output spectrum between points.

simplified speckle imaging equation [18], we processed the collected images to Speckle Flow Index (SFI) images. LSI methodology has been previously described in detail [17].

Experimental Design

Similar to previous publications [15,16], we used the dose-response analysis approach. We performed 40 experiments for IPL irradiation with either a single ($n = 13$), or double ($n = 27$) pulse of light. We monitor blood flow in a longitudinal fashion to study the fate of the microvasculature following phototherapy [19]. Raw speckle images were collected at the following time points: pre-phototherapy; immediately post-phototherapy; and at Days 1, 2, 3, and 7 after phototherapy. Five of the authors (BC, WJM, OCO, JDY, and JS) independently reviewed the SFI images collected on Day 7 of each experiment and graded each set of images on a binary scale: a "0" (no persistent vascular shutdown on Day 7) or "1" (persistent vascular shutdown achieved on Day 7) was assigned to each Day 7 image. We used a commercial software package (Prism version 5.0d, GraphPad Software, San Diego, CA) to perform a sigmoidal fit to the data and estimated a characteristic radiant exposure ($RE_{50/7}$) at which persistent vascular shutdown was achieved.

Monte Carlo Modeling

A Monte Carlo computational model incorporating the window chamber, multiple layers of tissue, and a flat circular source profile was developed to estimate the absorbed energy deposition in a vessel embedded within the hypodermis (Fig. 2). We simulated light propagation from 500 to 600 nm, in steps of 5 nm. The source was 5 mm in radius and assumed incident normal to a four-layer system comprised of skin, hypodermis, water and glass, to mimic the layers found in the window chamber. Within the hypodermis layer, a vessel with radius 81 μm was embedded. This vessel radius was selected based on calculation of the mean vessel radius determined from LSI images of 60 window chambers. The optical properties for each region are given in Table 1. The absorption coefficients for the skin, hypodermis and vessel were determined using the volume fractions of blood, water, blood oxygen saturation, and fat for each wavelength [20–22]. The scattering coefficient was determined from previous studies [20]. The Monte Carlo simulations were performed using used the Virtual Tissue Simulator software (http://virtualphotonics.codeplex.com). Photons were launched from the source and propagated within a conventional Monte Carlo simulation using discrete absorption weighting [23,24], which deposits absorbed energy at each collision. The tissue was subdivided into 10 μm × 20 mm × 10 μm voxels along the x-, y- and z-axes to collect the absorbed energy; in other words, the vessel was modeled as a cylinder of infinite length. For each simulation, 10^6 photons were used which ensured that the relative errors of the absorbed energy estimates within the vessel, due to statistical noise associated with Monte Carlo modeling, were less than 2%.

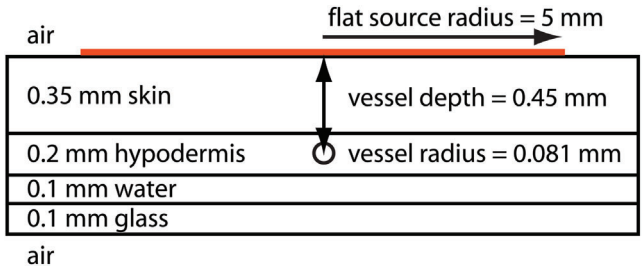

Fig. 2. Schematic of geometry used to represent the dorsal window chamber in Monte Carlo simulations. Not drawn to scale. A depth position of 0mm represents the air-skin interface. The center of the 0.081 mm radius vessel is at a depth of 0.45 mm.

TABLE 1. Tissue Properties Used in Monte Carlo Simulations. Anisotropy (g), Index of Refraction (n), Absorption (μ_α) and Scattering (μ_σ) Coefficients were based on values Obtained From Literature and are Wavelength Dependent

Region	g	n	μ_s/mm	μ_α/mm
Air	1	1.4	10^{-10}	0
Skin	0.81	1.44	λ-varied	λ-varied
Hypodermis	0.69	0.8	λ-varied	λ-varied
Water	1.0	1.33	0.5704	0
Glass	1.0	1.46	0.5704	0
Vessels	0.98	0.8	λ-varied	λ-varied

RESULTS

Single Pulse Narrowband IPL Irradiation

Similar to trends observed previously with photodynamic therapy [15] and PDL irradiation [16] of the microvasculature in the window chamber, we observed three trends in the single pulse narrowband IPL irradiation data (Fig. 3): (i) little to no change in blood flow over the 7 day monitoring period resulted in no persistent vascular shutdown; (ii) marked acute disruption in blood flow and vascular structure, followed by partial to full recovery of blood flow over the 7 day period, which also resulted in no persistent vascular shutdown; and (iii) immediate changes in blood flow and vascular structure, followed by prolonged and complete vascular shutdown by day 7. For experiments that did not result in persistent vascular shutdown, we observed the presence of hemorrhage within the window chamber 62% of the time (Table 2). Note that in Table 2, we present the data as irradiance (kW/cm^2) instead of radiant exposure, due to the different pulse durations used in this study. With an irradiance greater than 5333 kW/cm^2, we observed consistent, persistent vascular shutdown.

Double Pulse Narrowband IPL Irradiation

With double-pulse narrowband IPL irradiation, we observed the same three trends as described above for

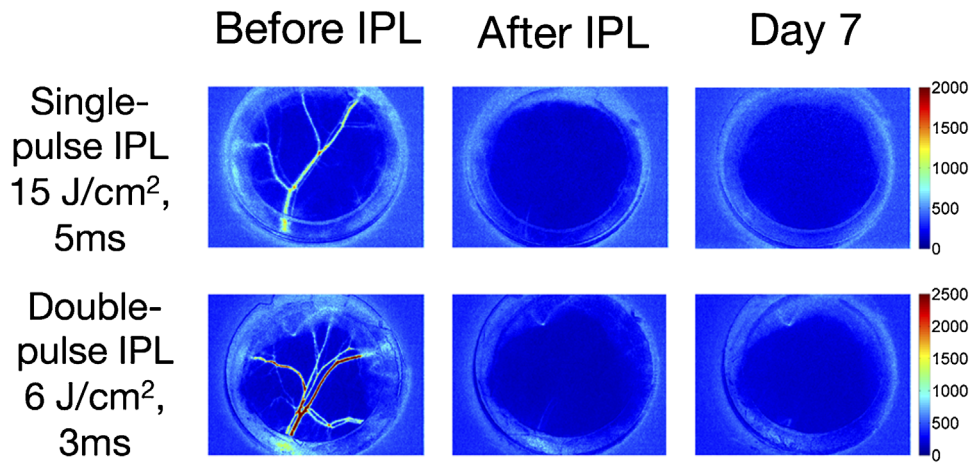

Fig. 3. Representative Speckle Flow index maps prior to and immediately after IPL irradiation, and at day 7. Image panels are shown for both single and double pulse protocols. Single-pulse irradiation was performed using a 15 J/cm^2 radiant exposure and 5 ms pulse duration, resulting in an irradiance of 3000 W/cm^2. Double-pulse irradiation was performed using a 6 J/cm^2 radiant exposure and 3 ms pulse duration, resulting in an irradiance of 2,000 W/cm^2. Persistent vascular shutdown was observed in both experiments.

TABLE 2. Summary of Observations of Persistent Vascular Shutdown for Experiments in Which the PDL Irradiance Was 2167–6667 W/cm^2, the Narrowband IPL Single Pulse Irradiance Was 2800–4000 W/cm^2, and the Narrowband IPL Stacked Pulse Irradiance Was 1250–2500 W/cm^2

PDL			Narrowband IPL-single			Narrowband IPL-stacked		
Irradiance	Hem.	Shutdown	Irradiance	Hem.	Shutdown	Irradiance	Hem.	Shutdown
2167	yes	0	2800	yes	1	1250	yes	0
2167	yes	0	3000	no	0	1250	yes	0
2667	yes	0	3000	yes	0	1400	yes	0
2667	yes	0	3000	no	1	1400	yes	0
3667	yes	0	3000	yes	0	1600	yes	0
4000	yes	0	3000	yes	1	1750	yes	0
4000	yes	0	3333	no	0	1750	yes	0
4333	yes	0	3333	no	0	2000	yes	1
4333	yes	0	3333	no	0	2200	yes	0
4667	yes	1	3333	yes	0	2200	yes	0
4667	yes	0	3333	yes	1	2400	yes	1
5000	yes	0	4000	yes	0	2500	yes	0
5000	yes	0	4000	yes	0	2750	yes	1
5333	yes	1				2750	yes	0
5333	yes	1				2750	yes	1
5333	yes	1				2800	yes	1
6667	yes	1				3000	yes	1
6667	yes	1				3000	yes	0
						3000	yes	0
						3333	yes	1
						3333	yes	0
						3333	yes	0
						3333	yes	1
						3667	yes	1
						3667	no	0
						3667	yes	1
						4000	no	0

The data also displays the shutdown response for each experiment at its corresponding irradiance, showing the relationship between increasing irradiance and persistent vascular shutdown. Hemorrhage formation was observed in all experiments in which persistent vascular shutdown occurred, but not all experiments in which hemorrhage formation occurred resulted in shutdown. A binary scale: a "0" (no persistent vascular shutdown on Day 7) or "1" (persistent vascular shutdown achieved on Day 7) was assigned to each Day 7 image.

the single pulse narrowband IPL irradiation data. We observed hemorrhage formation within the window chamber in 93% of experiments. Although hemorrhage formation did not correlate with persistent vascular shutdown, double pulse narrowband IPL irradiation induced persistent vascular shutdown at lower irradiance values (2000–4000 kW/cm^2) than single pulse irradiation (Table 2).

Monte Carlo Modeling

The results of the 20 simulations performed between 500–600 nm in 5 nm increments are displayed in Figure 4 A, for a single pulse IPL irradiation. Figure 4B shows a composite absorbed energy distribution from the narrowband IPL simulations, with weighted contributions from each wavelength dependent on the narrowband IPL spectrum, and the absorbed energy distribution from the 595 nm PDL simulation. Absorbed energy distribution is 53.2% higher in the top half of the composite narrowband IPL compared to the 595 nm (PDL).

Total absorbed energy distribution over the entire simulated vessel is 69.0% higher in the composite narrowband IPL compared to the 595 nm (PDL). We performed further analysis in Figure 4C, in which a line profile of the normalized total energy absorption profile at 595 nm was compared to the combined total absorbed energy of the narrowband IPL. With 595 nm irradiation, we observed that the average absorbed energy is more uniformly distributed over the diameter of the vessel than it is with narrowband IPL irradiation.

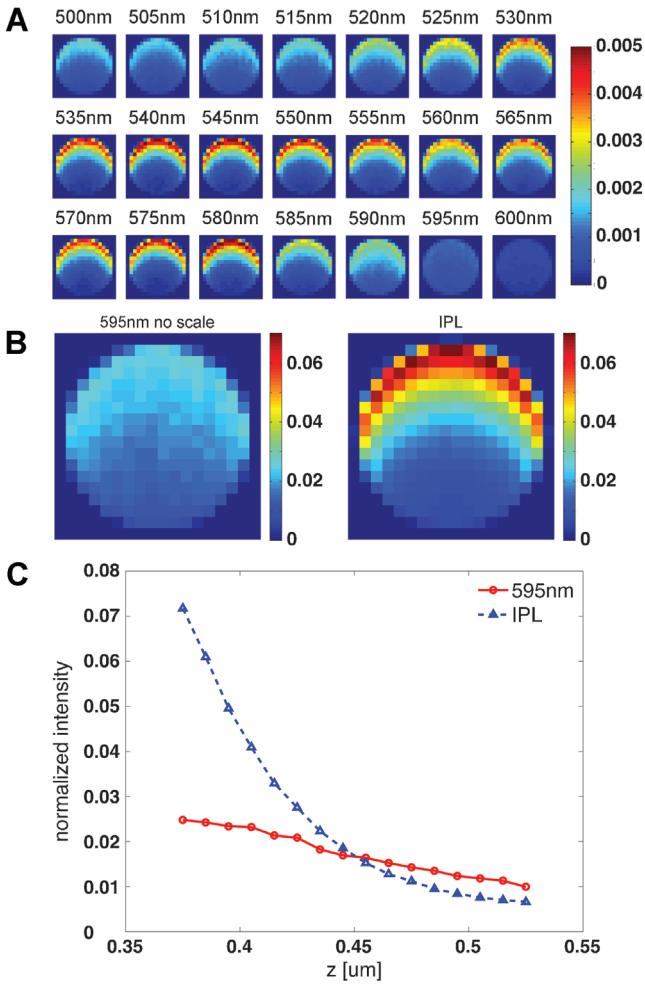

Fig. 4. (**A**) Normalized absorbed energy distribution within 0.081 μm radius vessel over 500–600 nm wavelength range at 5 nm increments. All energy distribution maps are plotted on the same color scale. (**B**) Comparison of 595 nm normalized absorbed energy distribution and composite narrowband IPL 500–60 nm energy distribution of 0.081 μm radius vessel. The average absorbed energy in the upper half of the line profile of the IPL is 0.0406 +/− 0.0004 while the average in the lower half is 0.0098 +/−0.0003. At 595 nm the average absorbed energy in the upper half is 0.0216 +/− 0.0004 and in the lower half is 0.0131 +/− 0.0003. Composite vessel indicates that most absorbed energy is contained within the top half of the vessel, while the bottom half has lower absorbed energy compared to 595 nm. (**C**) Line profile of normalized absorbed energy distribution with one-sigma error bars (bars are smaller than symbol) using 595 nm and narrowband IPL irradiation. With the former, the average absorbed energy is more evenly distributed over the entire vessel, as compared to the narrowband IPL absorbed energy.

DISCUSSION

Currently, the PDL is the gold standard technique in the treatment of PWS in the United States. On average, most patients typically require more than 15 sessions to achieve either a lightening of the PWS or complete removal [8]. Many groups [9–11,13,25] have studied the use of IPL as an alternate method to treat PWS birthmarks. Previous results have demonstrated limited efficacy due to a large variation of parameters including pulse width, output energy, and spectral output. Here, we studied the effects of these parameters for photothermal therapy using narrowband IPL and compared it with data from PDL experiments.

We previously characterized PDL irradiation in order to determine the radiant exposures necessary to achieve persistent vascular shutdown [16]. Utilizing similar methods described in previously published studies to photocoagulate the vasculature [15,26,27], we employed dose response analysis to determine the characteristic radiant exposure (7.1 J/cm^2) required to induce persistent vascular shutdown using 595 nm PDL irradiation.

Here, we characterized the narrowband IPL in single and double (stacked) pulse configurations. To more directly compare the results of PDL and narrowband IPL irradiation, we used irradiance values instead of radiant exposure. We found that the irradiance values associated with persistent vascular shutdown for both PDL and narrowband IPL irradiation were in the same general range (Table 2). For PDL irradiation, irradiance values greater than 4667 kW/cm^2 were required to induce perisistent vascular shutdown. For single pulse narrowband IPL, persistent vascular shutdown was induced with irradiances as low as 2800 kW/cm^2 and as high as 3333 kW/cm^2, but not in a consistent manner. Similarly, for double pulse narrowband IPL irradiation, persistent vascular

shutdown was observed at irradiances from 2000–3667 kW/cm^2, but a clear trend between increasing irradiance and occurrence of persistent vascular shutdown was not evident. Furthermore, with narrowband IPL irradiation, we were unable to identify a characteristic radiant exposure or irradiance required to achieve persistent vascular shutdown. Collectively, the data suggest that narrowband IPL irradiation with the parameters available in this specific IPL device, may cause persistent vascular shutdown at lower irradiances than the PDL, but in an inconsistent fashion.

Using double-pulse narrowband IPL irradiation, our data do not demonstrate a clear relationship between increasing irradiance and persistant vascular shutdown. This observation is consistent with other studies [13,28,29] in which a similar effect was observed of improved treatment outcome with an increasing number of pulses. One key difference between these studies and our present study is that they involved use of mulitple treatment sessions of multiple pulses, compared to our single use of double pulse narrowband IPL. Further study of this narrowband IPL deivce is warranted to test the hypothesis that multiple treatments involving multiple light pulses correlate to improved treatment outcome.

To understand better the observed difference between narrowband IPL and PDL irradiation, we performed Monte Carlo computational simulations to estimate the optical energy deposition in subdermal blood vessels. This required analysis of the output spectrum of the narrowband IPL for two purposes: (i) to quantify the wavelength dependent contributions towards the total absorbed energy in our Monte Carlo simulations and (ii) to calculate a weighted absorption coefficient at each wavelength along the spectrum. The weighted absorption coefficient was calculated by multiplying the oxyhemoglobin absorption spectrum [19] by the relative intensity of the narrowband IPL output spectrum. Over the range of 500–600 nm, we calculated a value of 149 cm^{-1}, which is nearly four times higher than the absorption coefficient (35 cm^{-1}) at 595 nm. A higher oxyhemoglobin absorption coefficient suggests that for a given irradiance, the narrowband IPL treatment should result in increased rate of energy deposition than PDL treatment. While simultaneously analyzing the weighted absorption coefficient, we compared experimentally observed treatment outcome results to those predicted by Monte Carlo computational simulation. Figure 4A shows the absorbed energy deposition on an average sized vessel (162 μm diameter) found in the dorsal window chamber model. While the modeling was performed using a simplified simulated geometry (i.e., the vessel in the window chamber is represented by a cylinder and each tissue layer has homogeneous absorption and scattering coefficients throughout its depth), we estimated the localized energy deposition within the vessel at different wavelengths. From 500 to 585 nm, the model predicts an energy deposition 53.2% higher at the top half of the vessel compared to the bottom half. At 595 and 600 nm, the total absorbed energy distribution is much more uniform, which can lead to more efficient conversion of light to heat.

Figure 4B shows the comparison between the combined total absorbed energy over all wavelengths, weighted by the intensity spectrum of the narrowband IPL. On the left side of Figure 4B, we see the total absorbed energy plot at only 595 nm. Due to the nature of the uniform and even energy distribution of the 595 nm, the PDL may be more effective in causing blood flow shutdown in the vessel because the temperature of the entire vessel is allowed to rise to a value associated with permanent damage [6]. This effect was demonstrated by Heger *et al*., who observed that inhomogenous photon distribution and subsequent subcritical temperature increase could be a source of incomplete photocoagulation within vessels, leading to a suboptimal treatment outcome.

Figure 4C shows a line profile of the normalized total energy absorption profile at 595 nm compared with combined total absorbed energy of the narrowband IPL. While the combined total absorbed energy of the IPL is higher in the top half of the vessel energy, we see an intersection point roughly half way into the vessel. Thus, as we move deeper into the combined total absorbed energy distribution, the absorbed energy drops off much more quickly compared to the 595 nm absorbed energy, which indicates that less energy is absorbed deeper into the vessel in narrowband IPL treatments compared to the PDL.

Collectively, based on our preclinical data (Table 2) and modeling data (Figure 4), we believe that further study is warranted to refine the narrowband IPL technology to treat PWS birthmarks. The incidence of PVS can be modulated with changes to the intensity spectrum, pulse durations, maximum radiant exposure, and alternate approaches beyond the single/double pulse protocol. The prevailing thought behind IPL usage to treat PWS birthmarks is that by using a broad range of wavelengths, absorption of the light during photothermolysis can be enhanced by absorption over the entire hemoglobin spectra. By calculating the weighted absorption coefficient at each wavelength, we can model the effects of broadband irradiation to study the full interactions between light dosimetry and treatment outcome. Additionally, the narrowband IPL can be further tuned to optimize a specific wavelength range that can be used to treat PWS, whereas the PDL only operates at discrete wavelengths.

ACKNOWLEDGMENTS

The work was supported in part by grants obtained from the National Institutes of Health (R01HD06636, K25EB007309), the National Institutes of Health Laser Microbeam and Medical Program (P41EB015890), the Arnold and Mabel Beckman Foundation, and the Undergraduate Research Opportunities Program at University of California, Irvine. The authors thank Alma Lasers for their generosity in providing us with the IPL device. The authors would also like to acknowledge Dr. Austin Moy (University of Texas at Austin) for guidance and assistance with preparation of this manuscript.

REFERENCES

1. Mulligan PR, Prajapati HJ, Martin LG, Patel TH. Vascular anomalies: Classification, imaging characteristics and implications for interventional radiology treatment approaches. Br J Radiol 2014;87(1035):20130392.
2. D Chen, Hu X-j, Lin X-x, G Ma, Jin Y-b, H Chen, W Li, Jiang C-h., Nodules arising within port-wine stains: A clinicopathologic study of 31 cases Am J Dermatopathol 33 2011; 144–151
3. Ashinoff R, Geronemus RG. Flashlamp-pumped pulsed dye laser for port-wine stains in infancy: Earlier versus later treatment. J Am Acad Dermatol 1991;24:467–472.
4. Waldorf HA, Alster TS, McMillan K, Kauvar AN, Geronemus RG, Nelson JS. Effect of dynamic cooling on 585-nm pulsed dye laser treatment of port-wine stain birthmarks. Dermatol Surg 1997;23:657–662.
5. Kelly KM, Nelson JS. Update on the Clinical Management of Port Wine Stains. Lasers Med Sci 2000;15:220–226.
6. Heger M, Beek JF, Moldovan NI, van der Horst CMAM, van Gemert MJC. Towards optimization of selective photothermolysis: Prothrombotic pharmaceutical agents as potential adjuvants in laser treatment of port wine stains A Theoreticaly Study. Thromb Haemost 2005;93:242–256.
7. Anderson RR, Parrish JA. Selective photothermolysis: Precise microsurgery by selective absorption of pulsed radiation. Science (New York, NY) 1983;220:524–527.
8. Koster PH, van der Horst CM, Bossuyt PM, van Gemert MJ. Prediction of portwine stain clearance and required number of flashlamp pumped pulsed dye laser treatments. Lasers Surg Med 2001;29:151–155.
9. Bjerring P, Christiansen K, Troilius A. Intense pulsed light source for the treatment of dye laser resistant port-wine stains. J Cosmet Laser Ther 2003;5:7–13.
10. Dong X, Yu Q, Ding J, Lin J. Treatment of facial port-wine stains with a new intense pulsed light source in Chinese patients. J Cosmet Laser Ther 2010;12:183–187.
11. Babilas P, Schreml S, Eames T, Hohenleutner U, Szeimies R-M., Landthaler M. Split-face comparison of intense pulsed light with short- and long-pulsed dye lasers for the treatment of port-wine stains. Lasers Surg Med 2010;42:720–727.
12. Adatto MA, Luc-Levy J, Mordon S. Efficacy of a novel intense pulsed light system for the treatment of port wine stains. J Cosmet Laser Ther 2010;12:54–60.
13. Li G, Lin T, Wu Q, Zhou Z, Gold MH. Clinical analysis of port wine stains treated by intense pulsed light. J Cosmet Laser Ther 2010;12(1):2–6.
14. Klein A, Bäumler W, Landthaler M, Babilas P. Laser and IPL treatment of port-wine stains: Therapy options, limitations, and practical aspects. Lasers Med Sci 2011;26:845–859.
15. Moy WJ, Patel SJ, Lertsakdadet BS, Arora RP, Nielsen KM, Kelly KM, Choi B. Preclinical *in vivo* evaluation of NPe6-mediated photodynamic therapy on normal vasculature. Lasers Surg Med 2012;44:158–162.
16. Kelly KM, Moy WJ, Moy AJ, Lertsakdadet BS, Moy JJ, Nguyen E, Nguyen A, Osann KE, Choi B. Talaporfin sodium-mediated photodynamic therapy alone and in combination with pulsed dye laser on cutaneous vasculature. J Invest Dermatol 2015;135:302–304.
17. Moy AJ, White SM, Indrawan ES, Lotfi J, Nudelman MJ, Costantini SJ, Agarwal N, Jia W, Kelly KM, Sorg BS, Choi B. Wide-field functional imaging of blood flow and hemoglobin oxygen saturation in the rodent dorsal window chamber. Microvasc Res 2011;82:199–209.
18. Ramirez-San-Juan JC, Ramos-Garćа R, Guizar-Iturbide I, Martínez-Niconoff G, Choi B. Impact of velocity distribution assumption on simplified laser speckle imaging equation. Optics Express 2008;16:3197–3203.
19. Choi B, Jia W, Channual J, Kelly KM, Lotfi J. The importance of long-term monitoring to evaluate the microvascular response to light-based therapies. J Invest Dermatol 2008;128:485–488.
20. Jacques SL. Optical properties of biological tissues: A review. Phys Med Biol 2013;58:R37–61.
21. Hale GM, Querry MR. Optical Constants of Water in the 200-nm to 200-microm Wavelength Region. Appl Opt 1973;12: 555–563.
22. van Veen RLP, Sterenborg HJCM, Pifferi A, Torricelli A, Chikoidze E, Cubeddu R. Determination of visible near-IR absorption coefficients of mammalian fat using time- and spatially resolved diffuse reflectance and transmission spectroscopy. J Biomed Opt 2005;10:054004.
23. Wang L, Jacques SL, Zheng L. MCML-Monte Carlo modeling of light transport in multi-layered tissues. Comput Methods Programs Biomed 1995;47:131–146.
24. Hayakawa CK, Spanier J, Venugopalan V. Comparative analysis of discrete and continuous absorption weighting estimators used in Monte Carlo simulations of radiative transport in turbid media. J Opt Soc Am A Opt Image Sci Vis 2014;31:301–311.
25. Reynolds N, Exley J, Hills S, Falder S, Duff C, Kenealy J. The role of the Lumina intense pulsed light system in the treatment of port wine stains-a case controlled study. Br J Plast Surg 2005;58(7):968–980.
26. Vargas G, Barton JK, Welch AJ. Use of hyperosmotic chemical agent to improve the laser treatment of cutaneous vascular lesions. J Biomed Opt 2008;13:021114.
27. Barton JK, Hammer DX, Pfefer TJ, Lund DJ, Stuck BE, Welch AJ. Simultaneous irradiation and imaging of blood vessels during pulsed laser delivery. Lasers Surg Med 1999;24:236–243.
28. Kuzmina I, Diebele I, Spigulis J, Valeine L, Berzina A, Abelite A. Contact and contactless diffuse reflectance spectroscopy: Potential for recovery monitoring of vascular lesions after intense pulsed light treatment. J Biomed Opt 2011;16: 040505.
29. B Wang, Y Wu, X Zhu, X-G Xu, T-H Xu, H-D Chen, Y-H. Li, Treatment of neck port-wine stain with intense pulsed light in Chinese population J Cosmet Laser Ther 15 2013; 85–90